

High-precision determination of universal amplitude ratios for the $q = 3$ Potts model in $2d$

Lev N. Shchur^{*,**}, Bertrand Berche^{**} and Paolo Butera^{***}

** Landau Institute for Theoretical Physics,
Russian Academy of Sciences,
Chernogolovka 142432, Russia*

*** Laboratoire de Physique des Matériaux,
Université Henri Poincaré, Nancy 1
BP 239, F-54506 Vandœuvre les Nancy Cedex, France*

**** Istituto Nazionale di Fisica Nucleare,
Sezione di Milano-Bicocca,
Piazza delle Scienze 3, 20126, Milano, Italia*

lev@landau.ac.ru,
berche@lpm.u-nancy.fr,
paolo.butera@mib.infn.it

May 6, 2019

Abstract

Monte Carlo (MC) simulations and series expansion (SE) data for the energy, specific heat, magnetization and susceptibility of the 3-state Potts model on the square lattice are analyzed in the vicinity of the critical point in order to estimate universal combinations of critical amplitudes. We estimate these amplitudes using the correction-to-scaling exponents predicted by conformal field theory. We also form effective ratios of the observables close to the critical point and analyze how they approach the universal critical-amplitude ratios. In particular, using the duality relation, we show analytically that for the Potts model with $q \leq 4$ states, the effective ratio of the energy critical amplitudes always approaches unity linearly with respect to the reduced temperature. This fact leads to the prediction of relations among the amplitudes of correction-to-scaling terms of the specific heat in the low- and high-temperature phases. We present numerical and analytical support for the form of the first two correction-to-scaling terms. Our results for the amplitude ratios closely agree with the theoretical predictions and the earlier numerical estimates of the specific-heat and the susceptibility amplitude-ratios.

1 Introduction

The universal character of appropriate combinations of critical amplitudes is an important prediction of scaling theory which in some cases still remains incompletely verified and subject to controversies. The concept of universality is very fruitful for the classification of the models and of the real physical systems undergoing phase transitions. The set of critical exponents and critical amplitudes describes the behavior of a system in the vicinity of the critical point. The universal combinations of critical amplitudes, together with the critical exponents, fully characterize the universality class [1]. The Potts model [2, 3], one of the paradigmatic models exhibiting continuous phase transitions is a good frame to reconsider the question of universal combinations of amplitudes. The universality class of the Potts model at its critical point is determined by the number of states q . The two-dimensional Potts models with three and four states can be experimentally realized as strongly chemisorbed atomic adsorbates on metallic surfaces at sub-monolayer concentrations [4] in accordance with the group-theoretical classification of the phase transitions of such systems [5–7]. Although critical exponents can be measured quite accurately for adsorbed sub-monolayers, confirming that these systems actually belong to the three-state [8] or to the four-state Potts model classes [9], it is unlikely that the low temperature LEED methods can be pushed [10] to determine also the critical amplitudes. Therefore, the numerical analysis of these models is the only available tool to check analytic predictions.

We shall restrict our analysis to the critical amplitudes and critical exponents which describe the behavior of the residual magnetization M , the reduced susceptibility χ , and the reduced specific heat C of the system at zero external field in the vicinity of the critical point

$$M(\tau) \approx B(-\tau)^\beta, \quad \tau < 0 \quad (1)$$

$$\chi_\pm(\tau) \approx \Gamma_\pm |\tau|^{-\gamma}, \quad (2)$$

$$C_\pm(\tau) \approx \frac{A_\pm}{\alpha} |\tau|^{-\alpha}. \quad (3)$$

Here τ is the reduced temperature $\tau = (T - T_c)/T$ and the labels \pm refer to the high-temperature and low-temperature sides of the critical temperature T_c . In addition to the above quantities, for the Potts models with $q > 2$ a transverse susceptibility can be defined in the low-temperature phase¹

$$\chi_T(\tau) \approx \Gamma_T (-\tau)^{-\gamma}. \quad (4)$$

For the 2D Potts model the critical exponents have been calculated exactly [11–14] in terms of the number of states q . Introducing the parameter y related to the number of states q of the model by

$$\cos \frac{\pi y}{2} = \frac{1}{2} \sqrt{q}. \quad (5)$$

¹In the following we will use the notations Γ_L and Γ_T for the longitudinal and transverse susceptibility amplitudes in the low temperature phase. Γ_- also used in the literature is identified to Γ_L .

we have for the thermal scaling dimension $x_\epsilon = (1 - \alpha)/\nu$

$$x_\epsilon = \frac{1 + y}{2 - y} \quad (6)$$

and for the magnetic scaling dimension $x_\sigma = \beta/\nu$

$$x_\sigma = \frac{1 - y^2}{4(2 - y)}. \quad (7)$$

The central charge of the corresponding conformal field theory is also simply expressed [14] in terms of y

$$c = 1 - \frac{3y^2}{2 - y}. \quad (8)$$

Analytical estimates of critical amplitude-ratios for the q -state Potts models with $q = 1, 2, 3$, and 4 were obtained by Delfino and Cardy [15]. They used the exact two-dimensional scattering field theory of Chim and Zamolodchikov [16] and estimated the ratios using a two-kink approximation for $1 < q \leq 3$ and the contributions from both the two-kink approximation and the bound state for $3 < q \leq 4$. This approximation leads to the value $c = 0.792$ for the central charge of the 3-state Potts model, for which the exactly known value is $c = 4/5$. Thus, the value of the central charge c is reproduced with an accuracy of one per cent. Using this approximate value in (8), we can calculate the scaling dimensions from (6)-(7) obtaining $x_\sigma = 0.1332$ and $x_\epsilon = 0.806$, which differ from the exactly known dimensions ($2/15$ and $4/5$ respectively) by less than one per cent.

The universal susceptibility amplitude-ratios Γ_+/Γ_L were calculated by Delfino and Cardy in [15]. Later Delfino, et al. [17] estimated analytically also the ratio of the transverse to the longitudinal susceptibility amplitude Γ_T/Γ_L . They obtained:

$$\Gamma_+/\Gamma_L \approx 13.848, \quad \Gamma_T/\Gamma_L \approx 0.327. \quad (9)$$

In the same paper [17], MC simulations were also reported which yield

$$\Gamma_+/\Gamma_L \approx 10, \quad \Gamma_T/\Gamma_L = 0.333(7). \quad (10)$$

In our previous paper [18], from the analysis of MC data and of old SE data for the 3-state Potts model, we estimated $\Gamma_+/\Gamma_L = 14 \pm 1$ in fair agreement with the theoretical prediction. The key point of our analysis was a fit including a correction-to-scaling term. Quite recently, these results were confirmed and substantially improved by Enting and Guttmann [19] who analyzed new longer series expansions derived by the finite lattice method. Their remarkably accurate estimates for the 3-state Potts model are:

$$\Gamma_+/\Gamma_L = 13.83(9) - 13.90(15), \quad \Gamma_T/\Gamma_L = 0.325(2) - 0.329(2). \quad (11)$$

In the present paper, devoted to the 3-state Potts model, we present new - more accurate - MC data supplemented by a reanalysis of the extended series derived by Enting and Guttmann [19]. We also present numerical and analytical support for the form of the first two correction-to-scaling terms.

We shall be concerned with the following universal combinations of critical amplitudes

$$\frac{A_+}{A_-}, \frac{\Gamma_+}{\Gamma_L}, \frac{\Gamma_T}{\Gamma_L}, R_C^+ = \frac{A_+\Gamma_+}{B^2}, R_C^- = \frac{A_-\Gamma_-}{B^2}, \quad (12)$$

where the last two are a consequence of the scaling relation² $\alpha = 2 - 2\beta - \gamma$. To the various critical amplitudes of interest, A_\pm, Γ_\pm, \dots , we have associated appropriately defined “effective amplitudes”, namely temperature-dependent quantities $A_\pm(|\tau|), \Gamma_\pm(|\tau|), \dots$, which take as limiting values, when $|\tau| \rightarrow 0$, the critical amplitudes A_\pm, Γ_\pm, \dots . By analogy, we also considered the “effective ratios” of some amplitudes, e.g., $A_+(\tau)/A_-(-\tau)$ which takes in the critical limit the value of the first amplitude ratio in the list (12). To avoid any risk of confusion, reference to these temperature-dependent quantities is always made with their explicit τ -dependence.

A central idea in our approach is to use the duality relation in order to improve the estimates of the effective amplitude-ratios measured at *dual* temperatures. In a first analysis, we also study directly the ratios of the effective amplitudes in (12) at symmetric reduced temperatures $\pm\tau$ above and below T_c . Better than separately estimating high- and low-temperature effective amplitudes, these effective ratios enable us to minimize correction-to-scaling effects in the accessible critical window. We also use the duality relation to estimate the leading correction-to-scaling amplitudes in the behavior of the specific heat and of the susceptibility. For this purpose, we compute ratios also on the duality line, e.g., the effective susceptibility amplitude ratio $\Gamma_+(\tau)/\Gamma_L(\tau^*) = \chi_+(\beta)/\chi_L(\beta^*)$ as the ratio of $\chi_+(\beta)$, the high-temperature susceptibility at the inverse temperature β , and $\chi_L(\beta^*)$, the low-temperature susceptibility at the dual inverse temperature β^* .

As a final result of our analysis, we estimate the susceptibility critical amplitude-ratios which, for $q = 3$, take the values $\Gamma_T/\Gamma_L = 0.3272(2)$ and $\Gamma_+/\Gamma_L = 13.83(8)$. These ratios are consistent with our previous results and with the predictions of Ref. [15].

2 Model and technical details

The Hamiltonian of the Potts model [2] reads as

$$H = - \sum_{\langle ij \rangle} \delta_{s_i s_j}, \quad (13)$$

where s_i is a “spin” variable taking integer values between 0 and $q - 1$, and the sum is restricted to the nearest neighbor sites $\langle ij \rangle$ on a lattice of N sites with periodic boundary conditions. The partition function Z is defined as usual by the sum over all spin configurations

$$Z = \sum_{conf} e^{-\beta H}. \quad (14)$$

²We refer the reader to Ref. [1] for a detailed discussion of the universality of the critical amplitude ratios.

with $\beta = 1/k_B T$, and k_B the Boltzmann constant (fixed to unity). On the square lattice in zero magnetic field, the model is self-dual. Denoting by β^* the dual of the inverse temperature β , the duality relation [2]

$$(e^\beta - 1)(e^{\beta^*} - 1) = q \quad (15)$$

determines the critical value of the inverse temperature $\beta_c = \ln(1 + \sqrt{q})$. From the duality transformation of the partition function $Z(\beta) = (q^{-1/2}(e^\beta - 1))^{2N} q^{-1} Z(\beta^*)$, a similar transformation follows for the internal energy density $E(\beta) = -N^{-1} \frac{d}{d\beta} \ln Z(\beta)$. The values $E(\beta)$ and $E(\beta^*)$ of the energy density at dual temperatures are thus related through (see, e.g., Ref. [20])

$$(1 - e^{-\beta}) E(\beta) + (1 - e^{-\beta^*}) E(\beta^*) = -2. \quad (16)$$

Dual reduced temperatures τ and τ^* can be defined by $\beta = \beta_c(1 - \tau)$ and $\beta^* = \beta_c(1 + \tau^*)$. Close to the critical point, τ and τ^* coincide through the first order, since $\tau^* = \tau + \frac{\ln(1+\sqrt{q})}{\sqrt{q}} \tau^2 + O(\tau^3)$.

2.1 Monte Carlo simulations

We use the Wolff algorithm [21] for studying square lattices of linear size L with periodic boundary conditions. Starting from an ordered state, we let the system equilibrate in 10^5 – 10^6 steps measured by the number of flipped Wolff clusters. The averages are computed over 10^6 – 10^7 steps. The random numbers are produced by an exclusive-XOR combination of two shift-register generators with the taps (9689,471) and (4423,1393), which are known [22] to be safe for the Wolff algorithm.

The order parameter of a microstate $\mathbf{M}(\mathbf{t})$ is evaluated during the simulations as

$$\mathbf{M} = \frac{qN_m/N - 1}{q - 1}, \quad (17)$$

where N_m is the number of sites i with $s_i = m$ at the time \mathbf{t} of the simulation [23], and $m \in [0, 1, \dots, (q - 1)]$ is the spin value of the majority of the spins. $N = L^2$ is the total number of spins. The thermal average is denoted by $M = \langle \mathbf{M} \rangle$.

Thus, the reduced longitudinal susceptibility in the low-temperature phase is measured by the fluctuation of the majority-spin orientation

$$\beta^{-1} \chi_L = \langle N_m^2 \rangle - \langle N_m \rangle^2 \quad (18)$$

and the reduced transverse susceptibility is defined in the low-temperature phase as the fluctuation of the minority of the spins

$$\beta^{-1} \chi_T = \frac{1}{q - 1} \sum_{\mu \neq m} (\langle N_\mu^2 \rangle - \langle N_\mu \rangle^2), \quad (19)$$

while in the high-temperature phase χ_+ is given by the fluctuations in all q states,

$$\beta^{-1} \chi_+ = \frac{1}{q} \sum_{\mu=0}^{q-1} (\langle N_\mu^2 \rangle - \langle N_\mu \rangle^2), \quad (20)$$

where N_μ is the number of sites with the spin in the state μ . Properly allowing for the finite-size effects, this definition of the susceptibility is, in both phases, completely consistent with the available series expansion data [18].

The internal energy density of a microstate is calculated as

$$\mathbf{E} = -\frac{1}{N} \sum_{\langle ij \rangle} \delta_{s_i s_j} \quad (21)$$

its ensemble average is denoted by $E = \langle \mathbf{E} \rangle$ and the reduced specific heat per spin is given by the energy fluctuations,

$$\beta^{-2} C = -\frac{\partial E}{\partial \beta} = (\langle \mathbf{E}^2 \rangle - \langle \mathbf{E} \rangle^2) N. \quad (22)$$

We have simulated the model on square lattices with linear sizes $L = 20, 40, 60, 80, 100$ and 200 . In each case, we have measured the physical quantities in a range of reduced temperatures called the ‘‘critical window’’ and defined as follows. Assuming a proportionality factor of order 1 in the definition of the correlation length, the relation $L \approx \xi \propto |\tau|^{-\nu}$ yields the value of the reduced temperature at which the correlation length becomes comparable with the system size L and thus below which the finite-size effects are not negligible. This value defines the lower end of the critical window. For example in the $q = 3$ case, for systems of sizes $L = 100$ and $L = 200$, we have $|\tau|_{min}(L = 100) \approx 0.004$ and $|\tau|_{min}(L = 200) \approx 0.0017$, respectively. The upper limit of the critical window is fixed for convenience as the value of the reduced temperature up to which the corrections to scaling in the Wegner asymptotic expansion [24] do not exceed a few percent, say 2–3%, of the leading critical behavior Eqs. (1-3).

2.2 Series expansions

Our MC study of the critical amplitudes will be supplemented by an analysis of the high-temperature (HT) and low-temperature (LT) expansions for $q = 3$ recently calculated through remarkably high orders by Briggs, Enting and Guttmann [19, 25]. In terms of these series, we can compute the effective critical amplitudes for the susceptibilities, the specific heat and the magnetization and extrapolate them by the current resummation techniques, namely simple Padé approximants (PA) and differential approximants (DA) properly biased with the exactly known critical temperatures and critical exponents.

The LT expansions, expressed in terms of the variable $z = e^{-\beta}$, extend through z^{46} in the case of the energy. The expansion of the longitudinal susceptibility extends through z^{71} . In the case of the transverse susceptibility the corresponding order is z^{53} . The magnetization expansion extends through z^{47} .

The HT expansions, computed in terms of the variable $v = (1 - z)/(1 + (q - 1)z)$, extend to v^{46} in the case of the energy, and up to v^{28} in the case of the susceptibility.

It is useful to point out that, for convenience, in Ref. [19] the product of the susceptibility by the factor $q^2/(q - 1)$, rather than the susceptibility itself, has been tabulated at HT because it has integer expansion coefficients. For the same reason, at LT the magnetization times $q/(q - 1)$ has been tabulated. Therefore the appropriate normalizations should be restored in order that the series yield amplitudes consistent with the MC results.

As a general remark on our series analysis, we may point out that in the $q = 3$ case, the accuracy of the amplitude estimates is good, due to the relatively harmless nature of the power-like corrections to scaling.

3 Critical amplitudes and universal ratios

3.1 Expected temperature-dependence of the observables

In the vicinity of the critical point, the reduced specific heat is generally expected to behave as

$$C(\tau) = \frac{A_{\pm}}{\alpha} |\tau|^{-\alpha} \mathcal{F}_{corr}(|\tau|^{\Delta}) + \mathcal{G}_{bt}(\tau), \quad (23)$$

where $\mathcal{F}_{corr}(|\tau|^{\Delta})$ is the correction-to-scaling function and $\mathcal{G}_{bt}(\tau)$ represents an analytic background (*bt* here stands for “background term”) which accounts for non-singular contributions to the specific heat, i.e. $\mathcal{G}_{bt}(\tau) = D_{\pm} + D'_{\pm}|\tau| + \dots$. The specific-heat and the leading correction-to-scaling exponents for $q = 3$ are given by $\alpha = 1/3$ and $\Delta = -\nu(D - x_{\epsilon_2}) = 2/3$ where $D = 2$ is the space dimension [26] and $x_{\epsilon_2} = (4 + 2y)/(2 - y)$ is the next-to-leading thermal exponent. In the HT phase and in the LT phase respectively, we can thus write³

$$C_+(\tau) = \frac{A_+}{\alpha} \tau^{-\alpha} (1 + a_{\Delta,+} \tau^{\Delta} + b_+ \tau + \dots) + D_+ + D'_+ \tau + \dots \quad (24)$$

$$C_-(-|\tau|) = \frac{A_-}{\alpha} |\tau|^{-\alpha} (1 + a_{\Delta,-} |\tau|^{\Delta} + b_- |\tau| + \dots) + D_- + D'_- |\tau| + \dots \quad (25)$$

where $a_{\Delta,\pm}$ is the amplitude of the leading correction-to-scaling, b_{\pm} is the next correction term and so on. In the correction-to-scaling factor the ellipse denotes terms in $|\tau|^{2\Delta}$, $|\tau|^{3\Delta}$, \dots , and also terms with an increasing sequence of other exponents [14] $\Delta' = -\nu(D - x_{\epsilon_3}) = 5\Delta$, $\Delta'' = -\nu(D - x_{\epsilon_4}) = 14\Delta$, etc. Other quantities should obey similar expansions including, beside the leading singularity, all corrections to scaling and background corrections,

$$\text{Obs.}(\pm|\tau|) \simeq \text{Ampl.} \times |\tau|^{\blacktriangleleft} \times (1 + \text{corr. terms}) + \text{backgr. terms}, \quad (26)$$

$$\text{corr. terms} = a|\tau|^{2/3} + b|\tau| + \dots, \quad (27)$$

$$\text{backgr. terms} = D_0 + D_1|\tau| + \dots \quad (28)$$

where \blacktriangleleft is a critical exponent which is known and depends on the observable considered.

3.2 Specific-heat critical amplitudes

Although duality determines exactly the ratio of the specific-heat amplitudes $A_+/A_- = 1$, it is instructive to define an efficient numerical procedure to compute this ratio. Moreover,

³Here and in the following, unless the contrary is stated, τ is defined as *positive*, but when the physical quantities are measured in the LT phase, $\tau = -|\tau|$, their temperature-dependence is explicitly denoted as $Q(-|\tau|)$.

the actual values of the amplitudes A_+ and A_- , albeit non-universal, are themselves informative, since they enter into other universal combinations, e.g. $R_c^\pm = A_\pm \Gamma_\pm / B^2$.

3.2.1 Corrections to scaling and background terms

It is not convenient to extract the critical amplitudes A_\pm directly from the specific heat. The energy density can be measured more accurately in the MC simulations, so in the following we shall study the dominant corrections to scaling and extract the background term from an analysis of the energy density.

In the HT phase and in the LT phase respectively, the energy can be conveniently written as

$$E_+(\tau) = E_0 + \frac{A_+}{\alpha(1-\alpha)\beta_c} \tau^{1-\alpha} (1 + a_{\Delta,+} \tau^\Delta + b_+ \tau + \dots) + D_+ \tau + \dots \quad (29)$$

$$E_-(-|\tau|) = E_0 - \frac{A_-}{\alpha(1-\alpha)\beta_c} |\tau|^{1-\alpha} (1 + a_{\Delta,-} |\tau|^\Delta + b_- |\tau| + \dots) + D_- |\tau| + \dots \quad (30)$$

The minus sign in front of $A_-/\alpha(1-\alpha)\beta_c$ is needed in order to recover, from the definition $C_-(-|\tau|) = \beta_c \partial E_- / \partial \tau = -\beta_c \partial E_- / \partial |\tau|$, the convenient specific heat amplitude $+A_-/\alpha$. The last term represents the analytic background which may be rewritten as $(A_\pm/\alpha(1-\alpha)\beta_c) |\tau|^{1-\alpha} d_\pm |\tau|^\alpha + \dots$, in order to be incorporated in the first sum,

$$E_\pm(\pm|\tau|) = E_0 \pm \frac{A_\pm}{\alpha(1-\alpha)\beta_c} |\tau|^{1-\alpha} (1 + a_{\Delta,\pm} |\tau|^\Delta + b_\pm |\tau| + \dots + d_\pm |\tau|^\alpha + \dots). \quad (31)$$

In Fig. 1 we have plotted the differences $\Delta E_+ = E_+(\tau) - E_0$ and $\Delta E_- = E_0 - E_-(-|\tau|)$ vs. the reduced temperature τ . These quantities are computed from both MC data (symbols) and SE (lines). By definition of the critical window, the finite-size corrections of the MC data are negligible in the range of reduced temperatures under study. Let us now define the effective amplitudes $A_+(\tau)$ and $A_-(-|\tau|)$ evaluated at symmetric reduced temperatures

$$A_+(\tau) = \alpha(1-\alpha)\beta_c (E_+(\tau) - E_0) \tau^{\alpha-1}, \quad (32)$$

$$A_-(-|\tau|) = \alpha(1-\alpha)\beta_c (E_0 - E_-(-|\tau|)) |\tau|^{\alpha-1}. \quad (33)$$

The re-summation of the series expansions of these effective amplitudes can be performed in various ways, all of which show a good convergence. We can compute each amplitude by simple PA's after performing the variable transformations $w = 1 - (1 - z/z_c)^\Delta$ in the LT case (or $w' = 1 - (1 - v/v_c)^\Delta$ in the HT case) in order to allow for the leading corrections to scaling. Completely consistent results are obtained by computing first-order inhomogeneous DA's of the amplitudes directly in the natural variables z and v .

According to Eq. (31), the arithmetic mean of the effective amplitudes $A_+(\tau)$ and $A_-(-|\tau|)$

$$\bar{A}(\tau) = \frac{1}{2} (A_+(\tau) + A_-(-|\tau|)) \quad (34)$$

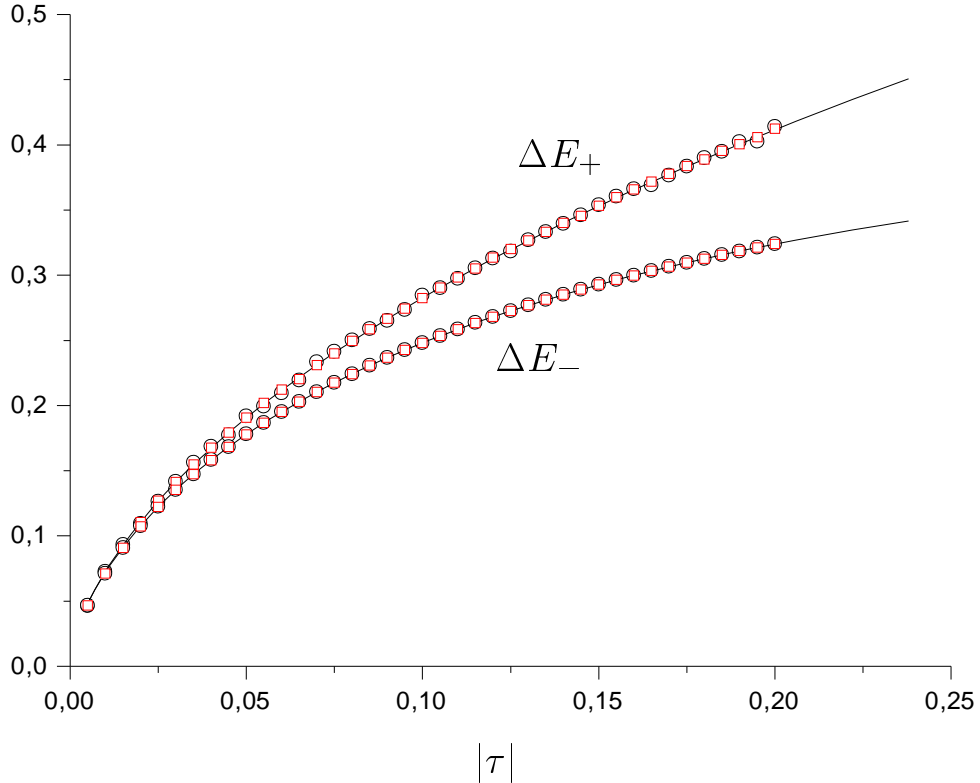


Figure 1: Energy differences ΔE_+ and ΔE_- , calculated from MC data for system sizes $L = 100$ (squares) and $L = 200$ (circles) and from SE data (continuous lines).

is expected to behave as

$$\bar{A}(\tau) = A \left(1 + \frac{A_+ d_+ + A_- d_-}{2A} \tau^\alpha \right) + O(\tau^\Delta) \quad (35)$$

where $A = \frac{1}{2}(A_+ + A_-)$ and the correction term comes from the leading correction to scaling in Eq. (31).

In order to compare Eq. (35) with the numerical data, we have plotted in Figure 2 the effective amplitudes $A_+(\tau)$, $A_-(-|\tau|)$ vs. $|\tau|^{1/3}$. The SE data for the mean $\bar{A}(\tau)$ are well represented asymptotically by the expression (solid line in Figure 2)

$$\bar{A}(\tau) \approx 0.399(2) - 0.283(1)\tau^{1/3}. \quad (36)$$

for $|\tau|^{1/3} > 0.16$ (which corresponds to the left boundary of the critical window as discussed above). This yields the estimate $A = 0.399(2)$. We can also conclude from the

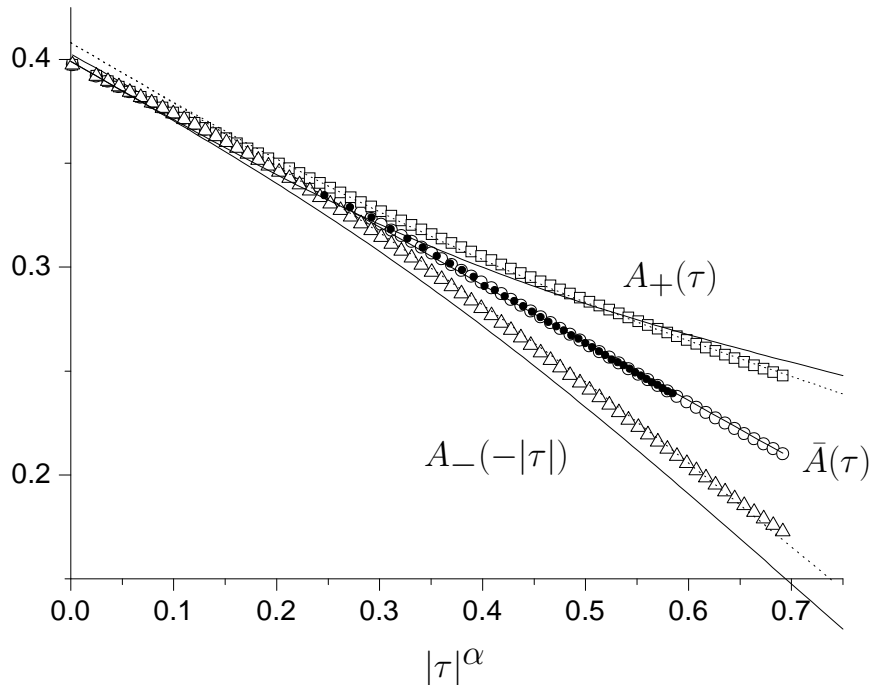


Figure 2: $A_+(\tau) = \alpha(1 - \alpha)\beta_c\Delta E_+\tau^{\alpha-1}$ (open squares) and $A_-(-|\tau|) = \alpha(1 - \alpha)\beta_c\Delta E_-|\tau|^{\alpha-1}$ (open triangles). Their arithmetic mean $\bar{A}(\tau)$ as computed from SE data (open circles), or from MC data (closed circles), together with the fits (solid lines: fit of SE data; dotted lines: fit of MC data).

essentially linear behavior of $\bar{A}(\tau)$ with respect to τ^α that the higher-order corrections are rather small. Therefore, we can empirically argue that $A_+a_{\Delta,+} \simeq -A_-a_{\Delta,-}$. Possibly also a cancellation of some higher order terms might occur in Eq. (34). This implies that the most important correction to be taken into account comes from the background term. It is necessary to include the additional terms $\pm 0.15|\tau|^2$ into Eq. (36) (obtained from the SE data) in order to catch the behavior at a larger distance from the critical point. This expression is more accurate also for smaller values of $|\tau|$ (not accessible through MC due to the finite size effects).

3.2.2 The effective amplitude-ratio $A_+(\tau)/A_-(\tau^*)$ on the dual line

The previous empirical observation of a cancellation of several correction-to-scaling terms in appropriate combinations of effective amplitudes can be restated more rigorously by duality arguments. We define effective amplitudes at dual values of the reduced temper-

ature⁴,

$$A_+(\tau) = \alpha(1-\alpha)\beta_c(E_+(\tau) - E_0)\tau^{\alpha-1}, \quad (37)$$

$$A_-(\tau^*) = \alpha(1-\alpha)\beta_c(E_0 - E_-(\tau^*))(\tau^*)^{\alpha-1} \quad (38)$$

and their ratio

$$\frac{A_+(\tau)}{A_-(\tau^*)} = \frac{(E_+(\tau) - E_0)\tau^{\alpha-1}}{(E_0 - E_-(\tau^*))(\tau^*)^{\alpha-1}} \quad (39)$$

the constant E_0 being the value of the energy at the transition temperature, $E_0 = E(\beta_c) = -1 - 1/\sqrt{q}$.

Using the asymptotic expansions Eqs. (29) and (30) in the duality equation Eq. (16) and expanding for small τ , we obtain an infinite set of relations among critical amplitudes, such as $A_+ = A_-$, $D_+ = -D_-$, $a_{\Delta,+} = a_{\Delta,-}$, $b_- = b_+ - 2\alpha_q$.. etc.. These equations hold for any $q \leq 4$. Therefore

$$\frac{A_+(\tau)}{A_-(\tau^*)} = 1 + (3-\alpha)\alpha_q\tau + O(\tau^{1+\alpha}) \quad (40)$$

with $\alpha_q = -E_0\beta_c e^{-\beta_c} = \frac{\ln(1+\sqrt{q})}{\sqrt{q}} \approx 0.5803$.

Hereafter we shall denote by A the common value of A_+ and A_- .

It is interesting to check numerically the validity of Eq. (40) for the asymptotic behavior of the ratio of effective amplitudes evaluated at *dual reduced temperatures*. The “direct division method” of HT and LT series suggested in Ref. [27] is very effective. It consists in computing the quotient of the $A_+(v)$ and the $A_-(z)$ series after taking $v = z$ (remember that $v_c = z_c$). This amounts precisely to compute the ratio of the effective amplitudes at dual temperatures. The quotient series thus obtained is resummed by simple PA’s or DA’s and can be extrapolated to the critical point obtaining the very accurate estimate $A_+/A_- = 1.000000(3)$. The results for $A_+(\tau)/A_-(\tau^*)$ shown in figure 3 are compared with the same ratio computed as function of the *symmetric reduced temperature* $|\tau|$, $A_+(\tau)/A_-(-|\tau|)$.

The fit of MC data at dual temperatures yields a value for the slope ≈ 1.5 which is not far from the expected value $8/3\alpha_q \approx 1.547$ of Eq. (40). The estimate of the same quantity in the case of symmetric reduced temperatures $|\tau|$ yields 1.38(1).

These plots show the *cancellation of the leading non-analytic correction to scaling in the ratio A_+/A_- of effective amplitudes*. We can now take advantage of this remark to improve the fit of the energy data, presented in the previous subsection. First, let us construct the mean of the effective amplitudes evaluated at dual reduced temperatures $\bar{A}_{\text{dual}}(\tau)$. For small τ the SE curve has the behavior (in perfect agreement with Eq. (36))

$$\bar{A}_{\text{dual}}(\tau) = 0.399(1) - 0.283(2)\tau^{1/3} \quad (41)$$

⁴Notice that, with our definitions, τ^* is positive and characterizes the LT phase.

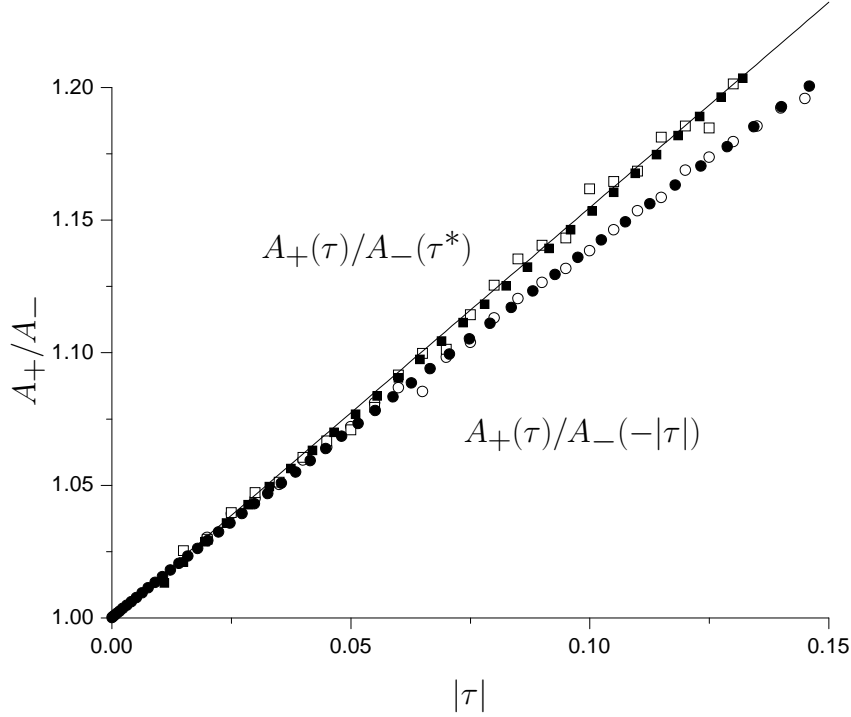


Figure 3: The effective-amplitude ratio $A_+(\tau)/A_-(-|\tau|)$ at *symmetric reduced temperatures*. The SE data are indicated by closed circles and the MC data by open circles. The ratio $A_+(\tau)/A_-(\tau^*)$ at *dual reduced temperatures* is denoted by closed squares in the case of the SE data and by open squares for the MC data. The solid line is the prediction Eq. (40).

As noticed above, the coefficient of the higher-order term $\tau^{2/3}$ is at least one order of magnitude smaller. In the linear approximation of the duality relation (40), $A_+(|\tau|)/A_-(\tau^*) \approx 1 + (3 - \alpha)\alpha_q\tau$, one has

$$A_{\pm}(\pm|\tau|) = \bar{A}_{\text{dual}}(\tau)(1 \pm (3 - \alpha)\alpha_q/2\tau). \quad (42)$$

Combining (41), (42) and using $(3 - \alpha)\alpha_q/2 \approx 0.774$, one gets

$$A_{\pm}(\pm|\tau|) \approx (0.399(1) - 0.283(2)\tau^{1/3})(1 \pm 0.774\tau). \quad (43)$$

These expressions are represented in Fig. 2 by the solid lines. In order to extend the SE data representation of Eq. (41) to larger values of $|\tau|$, we can add the next background correction term, estimated to be $\mp 0.15\tau^2$.

3.2.3 Energy and specific heat temperature dependence

From Eqs. (37), (38), (41) and (42), we get a numerical expansion of the energy of the 3-state Potts model:

$$\begin{aligned} E_+(\tau) - E_0 &= \frac{1}{\alpha(1-\alpha)\beta_c} \tau^{1-\alpha} \bar{A}(\tau) (1 + (3-\alpha)\alpha_q/2\tau) \\ &= 1.787(5)\tau^{2/3} (1 + 0.774(1)\tau - 0.412(4)\tau^{4/3}) - 1.269(9)\tau, \end{aligned} \quad (44)$$

$$\begin{aligned} E_0 - E_-(-|\tau|) &= \frac{1}{\alpha(1-\alpha)\beta_c} |\tau|^{1-\alpha} \bar{A}(|\tau|) (1 - (3-\alpha)\alpha_q/2|\tau|) \\ &= 1.787(5)|\tau|^{2/3} (1 - 0.774(1)|\tau| + 0.412(4)|\tau|^{4/3}) - 1.269(9)|\tau|. \end{aligned} \quad (45)$$

Note that the regular linear term appears through the combination of the $|\tau|^{1/3}$ correction in Eq. (41) with the leading singularity in $|\tau|^{1-\alpha}$.

As a conclusive test, we have plotted Eqs. (44) and (45) in figure 1, but they cannot be distinguished from the solid lines representing SE data.

We use expressions (45-44) to calculate the specific heat, and plot the results in the figure 4 together with the MC and SE data.

3.3 Susceptibility and magnetization amplitudes

3.3.1 The ratio Γ_T/Γ_L

The transverse and longitudinal reduced susceptibilities are expected to have the following asymptotic form in the LT phase [24]

$$\chi_T(-|\tau|) = \Gamma_T |\tau|^{-\gamma} \mathcal{F}_T(|\tau|^\Delta) + \mathcal{G}_T(|\tau|), \quad (46)$$

$$\chi_L(-|\tau|) = \Gamma_L |\tau|^{-\gamma} \mathcal{F}_L(|\tau|^\Delta) + \mathcal{G}_L(|\tau|), \quad (47)$$

where $\gamma = 13/9$ [14, 26] and the correction-to-scaling exponent $\Delta = 2/3$ is the same as above. For the purpose of the fit in the low temperature range accessible by our MC simulation, we shall use the following expansion of the reduced susceptibility

$$\chi(-|\tau|) = \Gamma |\tau|^{-\gamma} (1 + a_\Delta |\tau|^\Delta + a_{2\Delta} |\tau|^{2\Delta} + \dots + b|\tau| + \dots + d|\tau|^\gamma \dots), \quad (48)$$

where for simplicity, we choose a notation for the amplitudes of the corrections to scaling very similar to that adopted in the previous section, since there is no risk of confusion, and we incorporate the leading background term whose amplitude is denoted by d inside the main parenthesis. The ratio of the effective amplitudes $\Gamma_T(-|\tau|) = |\tau|^\gamma \chi_T(-|\tau|)$ and $\Gamma_L(-|\tau|) = |\tau|^\gamma \chi_L(-|\tau|)$ thus behaves as

$$\begin{aligned} \frac{\Gamma_T(-|\tau|)}{\Gamma_L(-|\tau|)} &= \frac{\Gamma_T}{\Gamma_L} (1 + (a_{\Delta,T} - a_{\Delta,L})|\tau|^\Delta + (b_T - b_L)|\tau| + \\ &\quad (a_{2\Delta,T} - a_{2\Delta,L} + a_{\Delta,L}^2 - a_{\Delta,T}a_{\Delta,L})|\tau|^{2\Delta} + (d_T - d_L)|\tau|^\gamma + O(|\tau|^{\Delta+1})). \end{aligned} \quad (49)$$

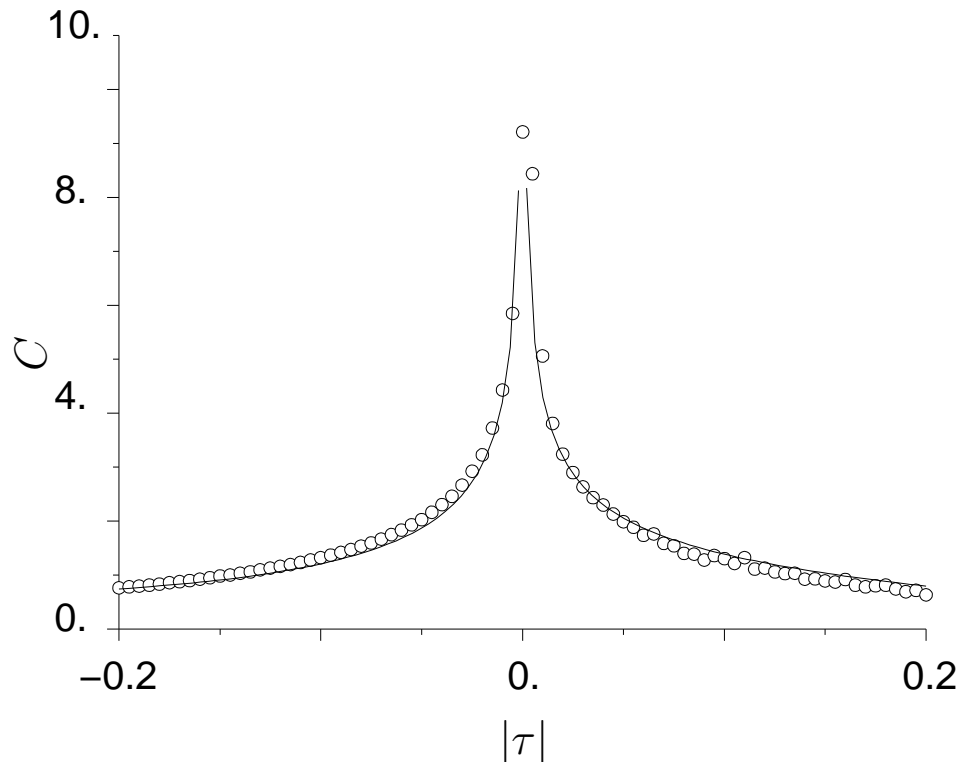


Figure 4: 3-state Potts model. MC data (open circles) and SE data (small solid boxes) for specific heat. The continuous line represents the specific heat calculated from Eqs. (44) and (45).

In Figure 5 we have represented the MC data for this effective ratio, plotted against the reduced temperature $|\tau|$. The data in Fig. 5 do not show any finite-size dependence even for the smallest lattice size, although their spread becomes obviously smaller for larger system sizes and longer MC runs. We performed a fit of the MC data collected for $L = 100$ and with the largest statistics (represented by closed circles in figure 5) to expression (49). The values of the parameters are reported in table 1 for different trial fits. It is worth noticing that, while the values of the parameters are sensitive to variations of the limits of the critical-region window, the amplitude ratio changes only within the error bars. Therefore the good quality of the MC data and the large size of the critical-region window enable us to estimate rather accurately the amplitude and the first correction term in the asymptotic expansion (49). In table 1, the leading correction comes from the regular term (last column) and the coefficient is clearly not negligible, therefore the fits # 2, 3 and 6 have our preference. Since it is hard to decide which one among the three is the most reliable, we consider that an average result $\Gamma_T/\Gamma_L = 0.327(1)$ is a safer value. Figure 5, if replotted as a function of $|\tau|^{2/3}$ shows a remarkably linear behavior for

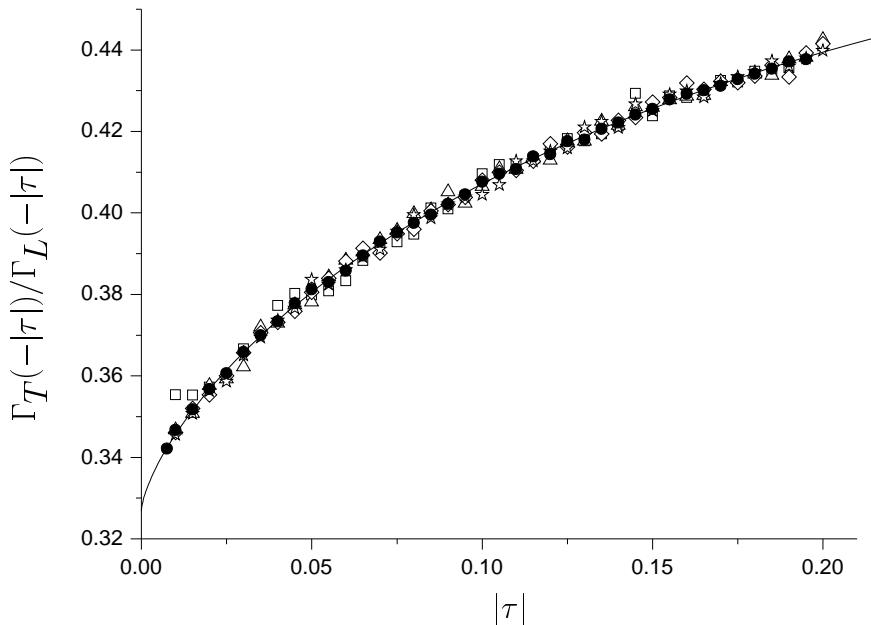


Figure 5: Effective ratio of amplitudes $\Gamma_T(-|\tau|)/\Gamma_L(-|\tau|)$ for lattices of linear sizes $L = 20$ (boxes), $L = 40$ (up triangles), $L = 60$ (down triangles), $L = 80$ (diamonds), $L = 100$ (stars) computed with $N_{MC} = 10^5$ Monte Carlo steps. We have indicated by closed circles the results of a computation on a $L = 100$ lattice with $N_{MC} = 10^6$ Monte Carlo steps. The dashed line (hardly visible) represents a fit of the data for $L = 100$ to Eq. (49). The values of the coefficients are listed in the last entry of table 1. The solid line represents the [22,22] Padé approximant to the ratio of the LT series in a conveniently transformed variable.

$|\tau|^{2/3} < 0.2$, while the result of the linear fit: $\Gamma_T/\Gamma_L = 0.329(1)$ supports our choice of the value $2/3$ for the leading confluent correction exponent.

Although possibly less accurate, the MC data for the low temperature susceptibilities can be fitted in the same window, leading to

$$\chi_T = 0.00409(2)|\tau|^{-13/9}(1 + 0.32(7)|\tau|^{2/3} - 1.88(11)|\tau|), \quad (50)$$

$$\chi_L = 0.01270(4)|\tau|^{-13/9}(1 - 1.60(5)|\tau|^{2/3} + 0.44(8)|\tau|). \quad (51)$$

The ratio of the amplitudes, $\Gamma_T/\Gamma_L \approx 0.322$, is fairly consistent with the value quoted above, but since no background term is included we consider that this value is not highly reliable. The differences between coefficients a_Δ 's and b 's appearing in Eq. (50) and (51) are also compatible with those quoted in table 1.

The quotient of the LT series for Γ_T and Γ_L can also be studied either most simply by

Table 1: Results of the fit to the MC data for the ratio Γ_T/Γ_L of the transverse and the longitudinal susceptibility in the critical region window. The absence of an entry in the table indicates that we have not included the corresponding parameter in the fit procedure.

Fit #	ratio		corrections coefficients		
	Γ_T/Γ_L	$\propto \tau ^\Delta$	$\propto \tau $	$\propto \tau ^{2\Delta}$	$\propto \tau ^\gamma$
1	0.328(2)	1.04(26)	1.11(87)	-2.03(79)	—
2	0.328(2)	1.13(23)	0.56(6)	—	-1.63(65)
3	0.327(2)	1.24(12)	—	1.9 ± 2.6	-3.1 ± 2.7
4	0.324(1)	1.71(5)	-1.10(7)	—	—
5	0.326(1)	1.37(2)	—	-1.02(6)	—
6	0.326(1)	1.33(2)	—	—	-1.08(6)

PA's in the transformed variable w as mentioned above or by DA's in the variable z . Both kinds of approximants are smoothly extrapolated to the value $\Gamma_T/\Gamma_L = 0.3272(2)$ for the critical amplitude ratio. The critical amplitudes can also be separately computed by DA's obtaining the estimates $\Gamma_T = 0.004166(5)$ and $\Gamma_L = 0.01273(1)$. Our results, summarized and compared with those of previous studies in Table 2 and 3, agree completely with the prediction $\Gamma_T/\Gamma_L = 0.327$ by Delfino, et al. [17] whose uncertainty is presumably of the order of a half percent.

3.3.2 The critical amplitude of the magnetization.

The magnetization is expected to behave in the critical region as

$$M(-|\tau|) = B|\tau|^\beta (1 + a_\Delta|\tau|^\Delta + \dots + b|\tau| + \dots) + D|\tau| + \dots, \quad (52)$$

where $\beta = 1/9$ is the magnetization exponent and as usually we have indicated only the leading corrections to scaling and the analytic background.

The analysis of the LT expansion for the effective amplitude $B(-|\tau|) = |\tau|^{-\beta}M(-|\tau|)$ of the magnetization can be efficiently performed either by simple PA's in the transformed variable w or by DA's. We obtain the estimate $B = 0.819(1)$ for the critical magnetization amplitude. DA's also indicate that the exponent of the leading correction to scaling is 0.73(3),

$$B(-|\tau|) = 0.819(1) - 0.226(2)|\tau|^{0.73(3)}. \quad (53)$$

Comparing (52) to (53) one can identify $|\tau|^{0.73(3)}$ with $|\tau|^\Delta$. As an illustration, a fit (with the exponent fixed to the value $\Delta = 2/3$) of the SE data is shown in the figure 6 (dotted line) and compared with the fit (53) (solid line).

A highly compatible fit is obtained for the MC data which yields

$$M = 0.818(1)|\tau|^{1/9}(1 - 0.65(3)|\tau|^{2/3} - 0.400(7)|\tau| + 0.2865|\tau|^{4/3}). \quad (54)$$

3.4 R_C^\pm ratios

We can finally estimate the value of the universal amplitude ratio $R_C^+ = A_+\Gamma_+/B^2$. If we use our estimates $A_+ = 0.399(1)$, $B = 0.819(1)$ and the value $\Gamma_+ = 0.176(1)$ obtained

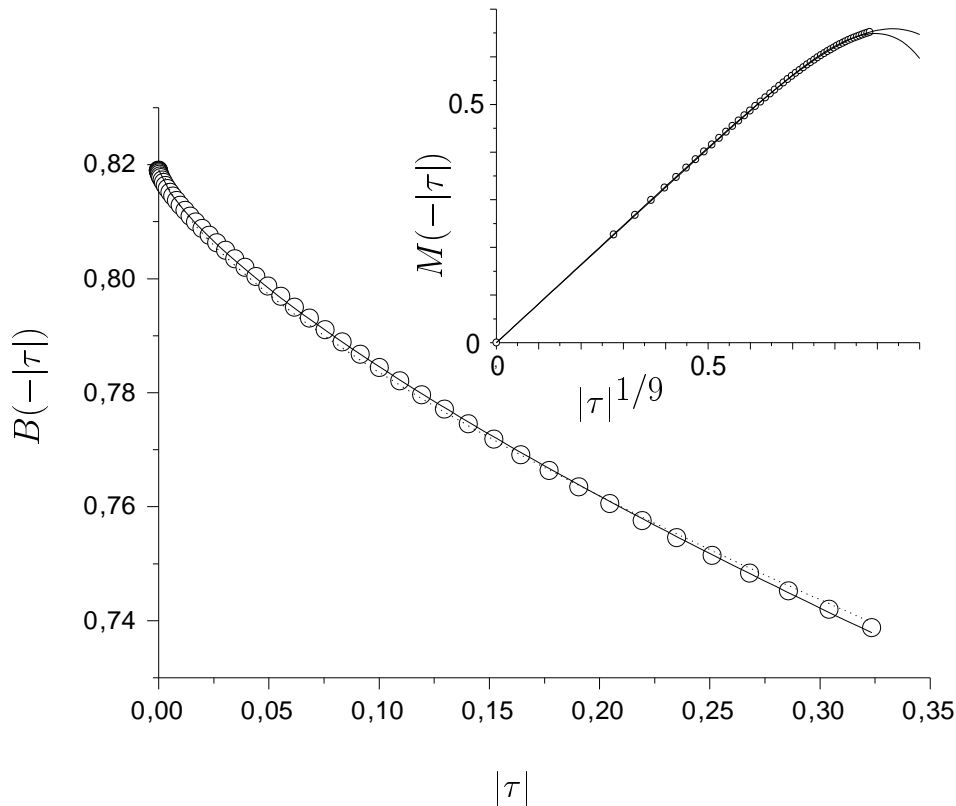


Figure 6: The effective amplitude of the magnetization M as computed from SE (open circles) together with the fits (lines, see in text). Insert: The magnetization M as function of $|\tau|^{1/9}$ (open circles) and a fit to the curves $B|\tau|^\beta(1 + a_M|\tau|^{\Delta_{\text{eff}}})$ with the exponent Δ_{eff} fixed to the values $\Delta_{\text{eff}} = \Delta = 2/3$ (upper line) and $\Delta_{\text{eff}} = 1 - \beta = 8/9$ (lower line).

from the presently available series [19] (much longer than those used in our previous study [18]), we conclude

$$R_C^+ = 0.1049(8).$$

This value compares very well with the estimate $R_C^+ = 0.1041$ by Delfino and Cardy [17].

The corresponding Monte Carlo estimates are $A_+ = 0.396(9)$, $B = 0.818(1)$ and $\Gamma_+ = 0.1783(7)$ leading to a value for the ratio $R_C^+ = 0.1054(29)$ consistent with SE estimation albeit less accurate.

An alternative approach, leading to a very similar numerical estimate $R_C^+ = 0.1043(8)$, consists in expressing R_C as the combination of the effective amplitudes $A(v)$, $\Gamma(v)$ and $B(z)$, after taking $v = z$, namely on the dual line in the $z - v$ plane. This procedure, however, wastes a large part of the available series coefficients.

Using the value $\Gamma_L = 0.01273(1)$ obtained from SE one can estimate $R_C^- = 0.00756(4)$ while using the MC value $\Gamma_L = 0.01270(4)$ one obtains $R_C^- = 0.00751(18)$. These values

agree well with Delfino and Cardy [17] analytic prediction $R_C^- = 0.00752$.

3.5 Summary of the results for the 3-state Potts model

By MC simulations and by series extrapolations, we have computed all universal amplitude-ratios studied in Refs. [15] and [17] for the $q = 3$ Potts model, with the exception of those involving the correlation length. We have shown that the cancellation of the leading non-analytic corrections to scaling in the ratio of the effective amplitudes of the energy evaluated at dual temperatures leads to a very accurate estimate of this amplitude ratio. Using this result, we have given an asymptotic numerical representation of the energy in a vicinity of the critical temperature, and observed that the main correction to scaling is due to the background term.

In table 2 we have collected the results from our fits of the main observables to the generic form given in Eq. (26). These fits are performed either using MC data or SE data, and their results are reported in the last column. From the estimates obtained, we can form the universal combinations reported in table 3. We have in general found more accurate results by fitting *effective amplitude ratios* rather than the amplitudes themselves. A comparison of our numerical results with the analytical predictions and with numerical estimates from other sources generally shows a very good agreement.

As a conclusion, we would like to mention that our primary interest is also to study the universal combinations of amplitudes in the case of the 4–state Potts model for which the available results are less convincing due to the presence of logarithmic corrections to scaling. We believe that the analysis proposed here in the case of the 3–state model (essentially based on an analysis of quantities at dual temperatures and of effective temperature-dependent combinations) can be successfully transposed to the 4–state case (see Refs. [28, 29] for preliminary results).

4 Acknowledgements

LNS is grateful to the Statistical Physics group of the University Henri Poincaré Nancy 1 for the kind hospitality. Both LNS and PB thank the Theoretical group of the University Milano–Bicocca for hospitality and support. Financial support from the twin research program between the Landau Institute and the Ecole Normale Supérieure de Paris and Russian Foundation for Basic Research are also acknowledged.

References

- [1] V. PRIVMAN, P.C. HOHENBERG, A. AHARONY, in *Phase Transitions and Critical Phenomena*, Vol. 14, edited by C. DOMB AND J.L. LEBOWITZ (Academic, New York, 1991).
- [2] R.B. POTTS, *Proc. Camb. Phil. Soc.* **48**, 106 (1952).
- [3] F.Y. WU, *Rev. Mod. Phys.* **54**, 235 (1982).

Table 2: Critical amplitudes and correction-to-scaling amplitudes for the 3–state Potts model, $\text{Obs.}(\pm|\tau|) \simeq \text{Ampl.} \times |\tau|^\Delta \times (1 + \text{corr. terms}) + \text{backg. terms}$. The results of the SE data analysis of Ref. [19] are tabulated together with our results obtained by combining the Monte Carlo and the SE data analysis. Results in bold face have our preference.

observable	amplitude	corrections			background		source
		$\propto \tau ^\Delta$	$\propto \tau $	$\propto \tau ^{2\Delta}$	$\propto \tau ^0$	$\propto \tau $	
$E_+(\tau)$	1.787(5)	$\simeq 0$	0.774(1)	-0.412(4)	E_0	-1.269(9)	this paper ^c
$E_-(- \tau)$	-1.787(5)	$\simeq 0$	-0.774(1)	0.412(4)	E_0	1.269(9)	this paper ^c
$C_+(\tau)$	A₊ = 0.399(1)	$\simeq 0$	1.548(3)	-1.236(12)	-1.269(9)	–	this paper ^b
	$A_+ = 0.396(9)$	–	–	–	–	–	this paper ^a
$C_-(- \tau)$	A₋ = 0.399(1)	$\simeq 0$	-1.548(3)	1.236(12)	-1.269(9)	–	this paper ^b
	$A_- = 0.396(9)$	–	–	–	–	–	this paper ^a
$\chi_+(\tau)$	$\Gamma_+ = 0.1783(7)$	0.24(2)	–	–	0.005(6)	–	[18]
	$\Gamma_+ = 0.1751(6)$	–	–	–	–	–	[19]
	$\Gamma_+ = 0.176(1)$	–	–	–	–	–	this paper ^c
$\chi_L(- \tau)$	$\Gamma_L = 0.012774(3)$	-1.517(8)	–	–	0.0070(2)	–	[18]
	$\Gamma_L = 0.01266(4)$	–	–	–	–	–	[19]
	$\Gamma_L = 0.01270(4)$	-1.60(5)	0.44(8)	–	–	–	this paper ^a
	$\Gamma_L = 0.01273(1)$	–	–	–	–	–	this paper ^c
$\chi_T(- \tau)$	$\Gamma_T = 0.004168(9)$	–	–	–	–	–	[19]
	$\Gamma_T = 0.00409(2)$	0.32(7)	-1.88(11)	–	–	–	this paper ^a
	$\Gamma_T = 0.004166(5)$	–	–	–	–	–	this paper ^c
$M(- \tau)$	$B = 0.819(1)$	–	–	–	–	–	this paper ^c
$M(- \tau)$	B = 0.818(1)	-0.65(3)	-0.400(7)	0.2865	–	–	this paper ^a

^a fit of MC data

^b derivative of Eqs. (44)-(45)

^c approximants of SE data

- [4] M. SOKOŁOWSKI AND H. PFNÜR, *Phys. Rev. Lett.* **49**, 7716 (1994).
- [5] E. DOMANY, M. SCHICK, J. WALKER, AND R.B. GRIFFITHS, *Phys. Rev. B* **18**, 2209 (1978).
- [6] E. DOMANY AND M. SCHICK, *Phys. Rev. B* **20**, 3828 (1979).
- [7] C. ROTTMAN, *Phys. Rev. B* **24**, 1482 (1981).
- [8] Y. NAKAJIMA, C. VOGES, T. NAGAO, S. HASEGAWA, G. KLOS AND H. PFNÜR, *Phys. Rev. B* **55**, 8129 (1997).
- [9] C. VOGES AND H. PFNÜR, *Phys. Rev. B* **57**, 3345 (1998).
- [10] H. PFNÜR, private communication.
- [11] M.P.M. DEN NIJS, *J. Phys. A* **12**, 1857 (1979).
- [12] R.B. PEARSON, *Phys. Rev. B* **22**, 2579 (1980).
- [13] B. NIENHUIS, *J. Stat. Phys.* **34**, 731 (1984); B. NIENHUIS, in *Phase Transitions and Critical Phenomena*, Vol. 11, edited by C. DOMB and J.L. LEBOWITZ (Academic Press, London, 1987).

Table 3: Universal combinations of the critical amplitudes in the 3–state Potts model. The first line shows the analytical predictions of Refs. [15] and [17]. The remaining lines are obtained by combining the Monte Carlo and series expansion (SE) data analysis (in particular, the second and third lines show the results of the SE data analysis of Ref. [19]).

A_+/A_-	Γ_+/Γ_L	Γ_T/Γ_L	R_C^+	R_C^-	source
1	13.848	0.327	0.1041	0.00752	[15] or [17]
	13.83(9)	0.325(2)	–	–	[19]
	13.90(15)	0.329(2)	–	–	[19]
	14(1)	–	–	–	[18]
1.000(1)	13.86(12)	0.322(3)	0.1049(29)	0.00748(18)	this paper ^a
–	13.83(9)	0.3272(7)	0.1044(8)	0.00753(4)	this paper ^b
1.000000(3)	–	0.327(1)	0.1038(8)	–	this paper ^c

^a from amplitudes extracted from fits of MC data quoted in table 2

^b from amplitudes extracted from fits of SE data quoted in table 2

^c from effective amplitude ratio, SE data, PA's or DA's

- [14] VL.S. DOTSENKO AND V.A. FATEEV, *Nucl. Phys. B* **240** [FS12], 312 (1984).
- [15] G. DELFINO AND J.L. CARDY, *Nucl. Phys. B* **519**, 551 (1998).
- [16] L. CHIM AND A.B. ZAMOŁODCHIKOV, *Int. J. Mod. Phys. A* **7**, 5317 (1992).
- [17] G. DELFINO, G.T. BARKEMA AND J.L. CARDY, *Nucl. Phys. B* **565**, 521 (2000).
- [18] L.N. SHCHUR, P. BUTERA, AND B. BERCHE, *Nucl. Phys. B* **620**, 579 (2002).
- [19] I.G. ENTING AND A.J. GUTTMANN, *Physica A* **321**, 90 (2003).
- [20] M. CASELLE, R. TATEO, AND S. VINCI, *Nucl. Phys. B* **562**, 549 (1999).
- [21] U. WOLFF, *Phys. Rev. Lett.* **62**, 361 (1989).
- [22] L.N. SHCHUR, *Comp. Phys. Comm.* **121-122**, 83 (1999).
- [23] K. BINDER, *J. Stat. Phys* **24**, 69 (1981).
- [24] F.J. WEGNER, *Phys. Rev. B* **5**, 4529 (1972).
- [25] K.M. BRIGGS, I.G. ENTING, AND A.J. GUTTMANN, *J. Phys. A* **27**, 1503 (1994).
- [26] B. NIENHUIS, *J. Phys. A* **15**, 199 (1982).
- [27] A.J. LIU AND M.E. FISHER, *Physica A* **156**, 35 (1989).
- [28] B. BERCHE, P. BUTERA AND L.N. SHCHUR, arXiv:0707.3317 [cond-mat.stat-mech]
- [29] L.N. SHCHUR, B. BERCHE AND P. BUTERA, *Europhys. Lett.* **81**, 30008 (2008).